Self-Assembled and Crystallized Composites Made from Poly(ether amine) and Montmorillonite in the Presence of Copper(II) Ions

Rong-Jer Lee,[1] Wei-Cheng Tsai,[2] Wen-Tung Cheng,[2] Bin-Chen Shiue,[2] Jiang-Jen Lin[3]

[1]*Material and Chemical Research Laboratories, Industrial Technology Research Institute, Hsinchu 31040, Taiwan*
[2]*Department of Chemical Engineering, National Chung Hsing University, Taichung 402, Taiwan*
[3]*Institute of Polymer Science and Engineering, National Taiwan University, Taipei 10617, Taiwan*

Received 3 November 2009; accepted 19 June 2010
DOI 10.1002/app.33001
Published online 29 September 2010 in Wiley Online Library (wileyonlinelibrary.com).

ABSTRACT: Self-assembled and crystallized composites made from montmorillonite (MMT) by intercalation with poly(ether amine) salts and copper(II) [Cu(II)] ions simultaneously were studied. The manipulation of the silicate unit structure of the secondary (001) lattice by physically imposed osmotic pressure on the platelet interlayer was used. Divalent copper salt assisted a strong depletion effect with balancing the counterions in the clay interlayer and resulted in the extension of the dimensions of the (001) plane by increasing the spacing expansion by more than two orders of magnitude. The simultaneous adsorption of Cu(II) and intercalation of poly(oxypropylene)-amine (POP) salts onto the MMT units ultimately minimized their amorphous aggregation through electrostatic attraction between the negative surface and positive edge among the silicate units. Alternatively, the attraction force through face-to-face stacking on the silicate surface is proposed, and the conformation of the POP/Cu(II) complex aligned with the approaching platelets to form orderly structures. X-ray diffraction of the MMT units exhibited a high order of reflection (i.e., (006)) in Bragg's pattern; this implied a repetitive regularity between the plate–plate distances. The high regularity disappeared when the Cu(II) adsorption exceeded the critical clay cation-exchange capacity of 1.4. The conformation of the flexible polyether backbone was altered and could no longer sustain the plate distance and the symmetric packing was destroyed when the basal spacing was decreased from 82.6 to 18.0 Å. J Appl Polym Sci 19: 3437–3445, 2011

Key words: metal–organic catalysts/organometallic; metal–polymer complexes; nanocomposites; nanotechnology; self-assembly

INTRODUCTION

Both organo–amine and inorganic metal salts can be used to swell clays through ion exchange for pillared silicates.[1,2] In previous studies, poly(oxypropylene)-amine (POP) has had a strong effect on the expansion of the basal spacing (*d*-spacing) and has formed well-dispersed hybrid organoclays.[3–6] The steric random coils of the polymers are assumed to be a major effect of the expansion of the *d*-spacing of the organoclays. The adsorption of the free-rotation polymeric molecular forms a polymer depletion layer on the solid flat silicate surface, and the depletion layer thickness (δ) on the particle surface is equal to the radius of gyration (R_g) of the bulky random coil of POP. When the polymer chains extend out of the particle surface, the particle is effectively separated by the depletion stabilizing effect. Hence, the most important factor for depletion stabilization is the molecular conformation of the adsorbed polymers. To analyze the interaction mechanism between the particle and polymer, experimental methods have been developed to measure δ. As mentioned in the literature, δ and the Debye length have been estimated indirectly by light scattering of the interaction between 6-μm polystyrene beads and the layered silicate[7] or by the rheological properties of colloid emulsions[8] and small-angle neutron scattering for colloid dispersions.[9]

The addition of a metal salt can impose an extra osmotic pressure effect on the polymer–particle dispersion system.[10,11] The relevant balance of the depletion layer structure may be altered in the presence of metal ions. In this study, three components, including polyether, copper(II) [Cu(II)] salt, and layered silicate clay, were used for model investigation. Smectite silicate is assumed to resemble a hard planar wall on a relative length scale, with a dimension ratio of the particle's diameter to the polymer R_g.[12–14] Layered silicate interacting with metal-ion polyether-backboned quaternary salts is the idealized model

Correspondence to: W.-T. Cheng (wtcheng@dragon.nchu.edu.tw) or J.-J. Lin (jianglin@ntu.edu.tw).
Contract grant sponsors: National Science Council of Taiwan, Ministry of Economic Affairs of Taiwan.

TABLE I
Poly(ether amine) Salt and Copper Salt for Clay Intercalation

Clay or intercalating agent	Chemical formula	Cation to exchange	Water solubility
Na^+-MMT	$Na_x(Al_{4-x}Mg_x)Si_8O_{20}(OH)_4$	Sodium	Dispersed
POP	$H_2NC_3H_6(OC_3H_6)_{33}NH_2$	Amine salt	Dispersed
POE	$H_2NC_3H_6(OC_3H_6)_a(OC_2H_4)_b(OC_3H_6)_cNH_2$ ($a + c = 5$, $b = 39.5$)	Amine salt	Soluble
Cu(II) sulfate	$CuSO_4$	Cu(II)	Soluble

for planar plate and sphere interaction. The polymeric complex of POP salt and copper sulfate was allowed to exchange ionically and intercalate with montmorillonite (MMT). The polymeric depletion layer was proposed to apply to the interlayer and also to the interparticles of the silicates. The osmotic pressure of the metal salts was expected to alter the crystalline morphology.

EXPERIMENTAL

This article presents a structural modification experiment on layered silicate[15–20] and polyelectrolyte consisting of POP salt and Cu(II) sulfate. The preparation of the organoclay is illustrated. A polymeric complex was formulated from POP [weight-average molecular weight (M_w) = 2000; 23.0 g, 11.5 mmol; Huntsman Chemical Co., Salt Lake City, Utah] and anhydrous Cu(II) sulfate ($CuSO_4$; 1.8 g, 11.5 mmol, Showa Chemicals, Tokyo, Japan); these were mixed and stirred 1 h to form a clear blue solution with a POP/Cu(II) molar ratio of 1.0/1.0. Ten grams of the Na^+ form of MMT [Na^+-MMT; cation-exchange capacity (CEC) = 1.15 mequiv/g; Paikong Nano Co., Taoyuan, Taiwan] was vigorously dispersed in 1 L of deionized water at 80°C. The slurry was added to the polymeric complex solution, and after the mixture was vigorously stirred at 80°C for 5 h, a brown precipitate was collected at ambient temperature, washed three times with toluene/ethanol (1/1 v/v), and filtered to eliminate unreacted reactants. The precipitate was dried at 80°C for 12 h. With a similar process, MMT was intercalated with polyoxyethylene amine (POE; M_w = 2000; 23 g, 11.5 mmol; Huntsman Chemical Co.).

The POP- and POE-modified clays were used to compare their hydrophobic effects on the self-assembly. These polyether amines and MMT materials are listed in Table I.

Various concentrations of POP and copper sulfate were allowed to intercalate with MMT to obtain different organosilicates. Copper sulfate was added in increasing amounts to form polymeric complexes [POP/Cu(II)] with molar ratios of 1.0/0, 1.0/0.1, 1.0/0.3, 1.0/0.5, 1.0/1.0, 1.0/1.25, and 1.0/1.65. The resulting *d*-spacing and compositions were correspondingly altered, as shown in Table II.

The organosilicate crystals were further dried at 80°C for 5 h before the experimental analysis. Scanning electron microscopy (SEM; Topcon ABT-150S, Tokyo, Japan) was used to investigate the microstructure of the organoclays. Wide-angle X-ray diffraction (XRD; Shimadzu, Kyoto, Japan) at 30 kV and 20 mA was used with nickel-filtered Cu Kα radiation to determine the *d*-spacing of the polyether/copper salt intercalated MMT. The XRD data were used to characterize the silicate crystalline structure.[21,22]

The organic components adsorbed on silicates were determined by thermogravimetric analysis (Seiko model SSC/5200, Chiba, Japan) under air flow. We determined the weight loss by heating the sample up to 800°C to burn the organics. Hydrated water confined in silicates was measured at 100°C heating. The chemical compositions of the hybrid polyelectrolytes were estimated with a PerkinElmer Paragon 500 Fourier transform infrared (FTIR) spectrophotometer (Waltham, Massachusetts) in 4000–400-cm^{-1} range, for the solid sample in KBr pellets with a 4-cm^{-1} resolution. The metal-ion concentration was determined with inductively coupled plasma (Spectro Analytical Instruments, Flame-p, Duisburg, Germany) to measure the cation content. The samples for analysis were fully dried and pulverized into a fine powder, and

TABLE II
Intercalating Agents and Interlayer Spacing of Intercalated MMT

Intercalating agent	*d*-Spacing (Å)	Organic content (wt %)[a]	Copper content (wt %)[b]
Cu(II)	14.0	—	5.80
POE	19.4	43	—
POP	58.0	56	—
1.0/0.1 POP/Cu(II)	80.1	55	0.25
1.0/0.3 POP/Cu(II)	80.8	—	—
1.0/0.5 POP/Cu(II)	80.0	52	1.20
1.0/1.0 POP/Cu(II)	82.6	61	—
1.0/1.25 POP/Cu(II)	80.0	51	2.34
1.0/1.65 POP/Cu(II)	17.8	32	—

[a] Measured with thermogravimetric analysis.
[b] Measured with inductively coupled plasma.

the powder samples were heated to melt at 1000°C. The melt samples were dissolved in HF, HNO, and $HClO_4$ acids, and we measured the metal-ion contents by analyzing their specific absorption spectra.

RESULTS AND DISCUSSION

Coordination reaction on the silicate surface

The formation of a solid deposition from a suspension state is usually due to anisotropic agglomeration in a random orientation.[23–25] To obtain an orderly alignment of a layered clay, a second interrupting force is required for the new stage of thermal stability.[26] With the self-assembling tendency, an orderly clay–polymer crystal was prepared by depletion effects by the combination of the metal salt and POP chain entanglement through ionic tethering on the silicate surface. Monovalent sodium ions of silicate were expelled from the interlayer spacing, as the polymeric complex of POP quaternary salt and divalent Cu(II) were cointercalated onto the layered silicate. The sodium concentration of Na^+-MMT decreased from 2.5 to 0.1 wt % after 1.0 CEC of POP adsorption. In this study, the intercalation was a process of cationic exchange reaction[27] and was followed by organic embedding into the clay gallery. Brown crystals of the dispersed organoclay intercalated with the POP/Cu(II) at 1.0/0.5 were collected from the blue solution. Hydrated divalent Cu(II) was blue as a residual in the water medium. The brown color of the products implied a coordination involving Cu(II),[28] in which 2 equiv of amine and anionic SiO^- were combined with the Cu(II) of $(POP{-}NH_2)_2Cu^{2+}(MMT{-}SiO^-)_2$ on the surface of silicates. The formation was evidenced by the FTIR (KBr) vibration band of $-NH_3^+$ at 3280 cm^{-1} for POP/MMT, which disappeared with the Cu(II) association in the POP/Cu(II)/MMT composite.[29] As shown in Figure 1, the hydronium HO stretching band at 1725 cm^{-1} was a product of proton (or cationic ion) exchange between Cu(II) coordinated water and ammonium in the confined silicate layers.[30]

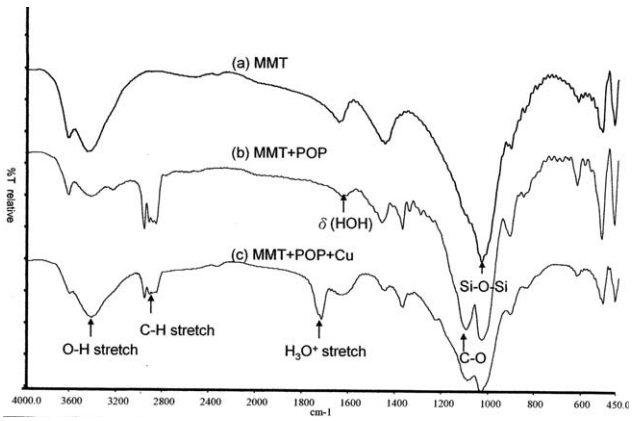

Figure 1 FTIR spectra of (a) MMT, (b) MMT/POP, and (c) MMT/POP/Cu (T = transmittance). The hydronium stretching band at 1725 cm^{-1} is a product of proton (or cation-ion) exchange between Cu(II)-coordinated water and polymeric ammonium in the confined silicate layer.

Secondary structures of the crystalline organoclay

The morphology of the modified organoclays was analyzed by SEM, and a specific secondary crystallization of the silicates was observed with the dimensions of silicate plates extending tremendously for more than two orders. In additional, a new organoclay crystalline with a 10-μm length was produced from the intercalated hybrid product of POP/Cu(II) combining with MMT, which was originally aggregated as micrometer size from the 100–150 nm primary particles.[15,16] In contrast to the edge–face aggregated structure,[31] the POP/Cu(II)/MMT hybrid was found to form self-assembled crystals in water. The organically modified hybrids avoided the agglomeration of edge–face attraction, as sketched in Figure 2(a), but self-assembled through face-to-face stacking into an ordered structure in the bulk, as shown in Figure 2(b). Therefore, the osmotic pressure exerted on the organoclays exerted by the depletion effect of Cu(II) ions was proposed to contribute the expansion in the (001) direction, and the addition of 1 molar ratio of Cu(II) to POP clay increased the d-spacing of the POP clay by 43%, as shown in Table II. The effect of the Cu(II) ionic osmotic pressure was explained by the comparison of the d-spacing and copper element analysis of the 1.0/1.0 POP/Cu(II) sample to clay and the POP clay sample without Cu(II).

The crystal structure was analyzed by XRD, as shown in Figure 2(c), and the XRD pattern of Figure 2(d) refers to the 1.0/1.0 POP/Cu(II) sample in Table II. The assignment of the order of reflection (n) of the X-ray powder diffractogram involved the identification and semiquantification of the characteristic crystalline peaks in the sample,[22] and there were n values of 3–6 on the (001) lattice assigned to POP/Cu(II)/MMT. According to Bragg's law, n was determined as follows:

$$n = (2d\sin\theta)/\lambda \quad (1)$$

where λ is the wavelength defined by Cu Kα and θ is the reflection angle. The Fraunhofer constructive diffraction intensity of one-dimension (I) was calculated as follows:

$$I = I_0[\sin(\Phi + \pi/2)/\Phi]^2 \quad (2)$$

where I_0 is intensity of incident light, Φ is the phase difference of the diffraction rays. At the peak maximal intensity, Φ was calculated as follows:

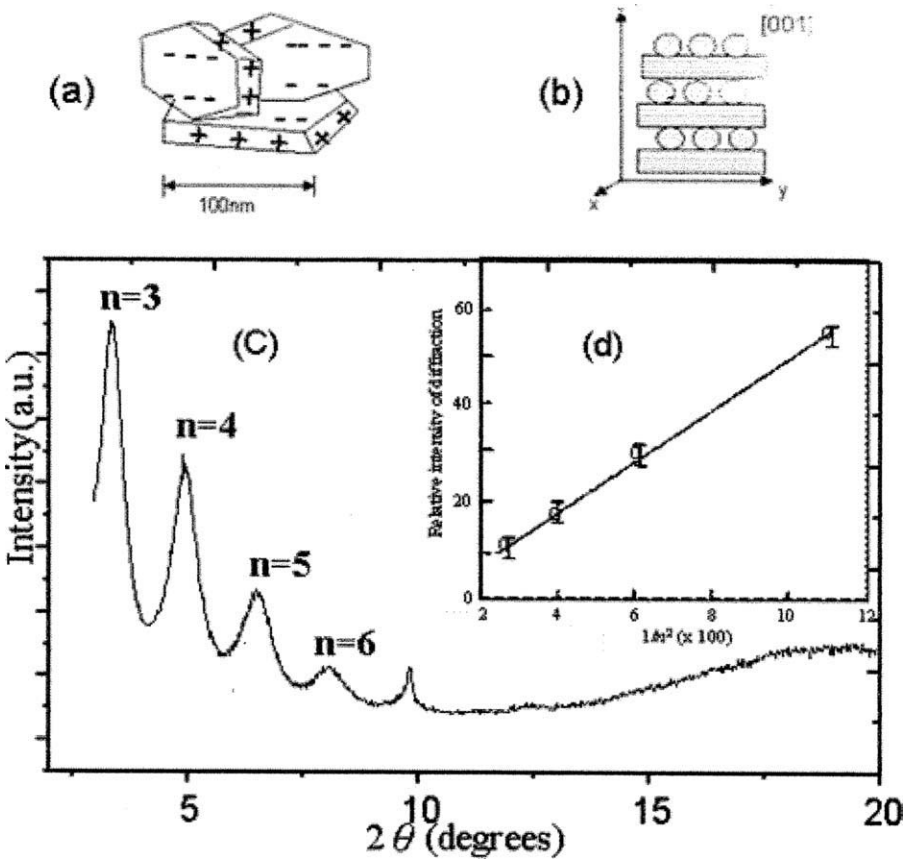

Figure 2 (a) Illustration of the edge–face aggregated structure of clay, (b) self-assembly through face-to-face stacking into an ordered structure for modeling the orderly XRD pattern of Cu(II) and POP intercalated clay, (c) XRD pattern of the self-assembled organoclay, and (d) relative peak intensity of XRD as a function of n.

$$\Phi = (2\pi d \sin\theta)/\lambda = n\pi \quad (3)$$

where I, corresponding to n, is proportional to a function of a constant of illumination (k):

$$I = k/n^2 \quad (4)$$

A calibration line of the peak intensity and n values from 3 to 6 is shown in Figure 2(d). The linear relationship of the relative intensity was well matched to the peak assignment. The crystal growth showed extremely orderly packing in the (001) direction, and the d-spacing was 82.6 Å.

The wide spacing and excellent symmetry on the (001) lattice of POP/Cu(II)/MMT implied a narrow distribution of polymer conformation within the silicate interlayer. In an aqueous solution, hydrophobic POP, which was attached on a silicate surface, has high tendency to aggregate and create a depletion layer to separate the particles. The conformation of the intercalated polymer species in expanded silicates is understood primarily through recent molecular modeling and neutron scattering studies.[8,9] The high surface area of the swollen MMT provides an ideal two-dimensional plate for polymer interaction and assumed similarity to plate and sphere interaction. For POP and Cu(II) coordinating with anionic silicates, the silicate d-spacing was equal to the diameter of the polyether random coil[3]:

$$d = 2R_g \quad (5)$$

The molecular conformation of the adsorbed polymer defined the spacing expansion of the layered silicate.

POP in the silicate could extend its steric conformation coil out of the silicate surface and widely separate the two plates; the 33 propylene oxide unit of the backbone effectively contributed to the volume restriction of the depletion layer.

Two stages of surface adsorption and d-spacing expansion

For POP-intercalated MMT with molecular weights of 400 and 4000, the d-spaces were 19.4 and 92.0 Å, respectively, as previously reported.[22,32–34] The d-spacing increased linearly and proportionally with the polymer molecular weight. However, the loading amount of the polymer did not affect the d-spacing

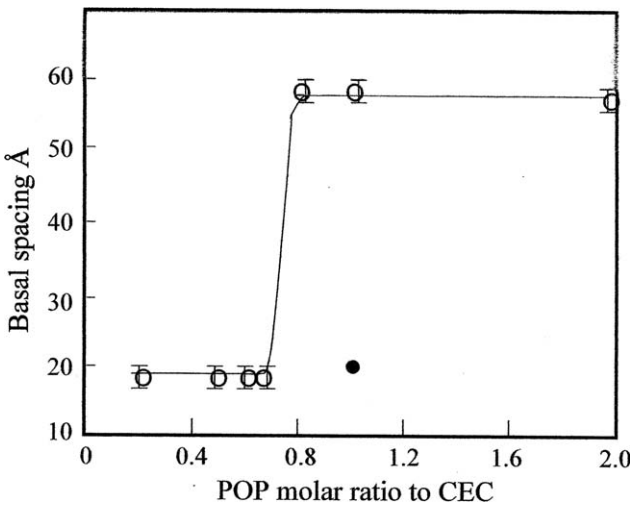

Figure 3 (○) *d*-Spacing expansion of different POP loadings and (●) *d*-spacing of POE intercalation.

expansion before the surface adsorption was saturated. For the POP (M_w = 2000)/MMT samples containing amine/CEC ratios of 0.2, 0.5, 0.6, and 0.65, the intercalated MMTs were analyzed to be 17.8, 18.0, 18.4, and 18.3 Å, accordingly.[22] When the ratio fractions were 0.8, 1.0, and 2.0, the wide gallery spacings encapsulating POP were 58.0, 58.0, and 57.0 Å, respectively. As shown in Figure 3, the intercalation reaction of POP/MMT should have had two stages: the first one was surface adsorption without a significant *d*-spacing extension. In this stage, water molecules were filled into the cell gap of silicate, and *d*(001) was clearly around 18.0 Å. In the second stage, POP was adsorbed into the gallery, and *d*(001) expanded to 58 Å. With further loading of POP beyond 0.8 CEC, the *d*-spacing showed no further expansion. It was the conformation of the intercalated polymer that affected the extension of *d*-spacing.

The POP and Cu(II) cointercalation into layered silicate also affected the *d*-spacing and orders of symmetry. Both the chemical and physical characteristics of Cu(II) ions were expected to affect the gallery of pillared MMT. As shown in the FTIR spectra, the POP/Cu(II)/silicate system was characterized to have IR bands involving the coordination reaction among silicates, Cu(II), and amine salts. The *d*-spacing and symmetry of the organoclays, depending on the amount of Cu(II) present in the system, were analyzed by XRD. The osmotic pressure of dissolved Cu(II) ions acted on the plates of the organoclays by a face-to-face piling and, hence, may have initiated a crystallization process. A high epitaxial (001) self-assembly of POP/Cu(II)/MMT with Bragg peaks of *n*

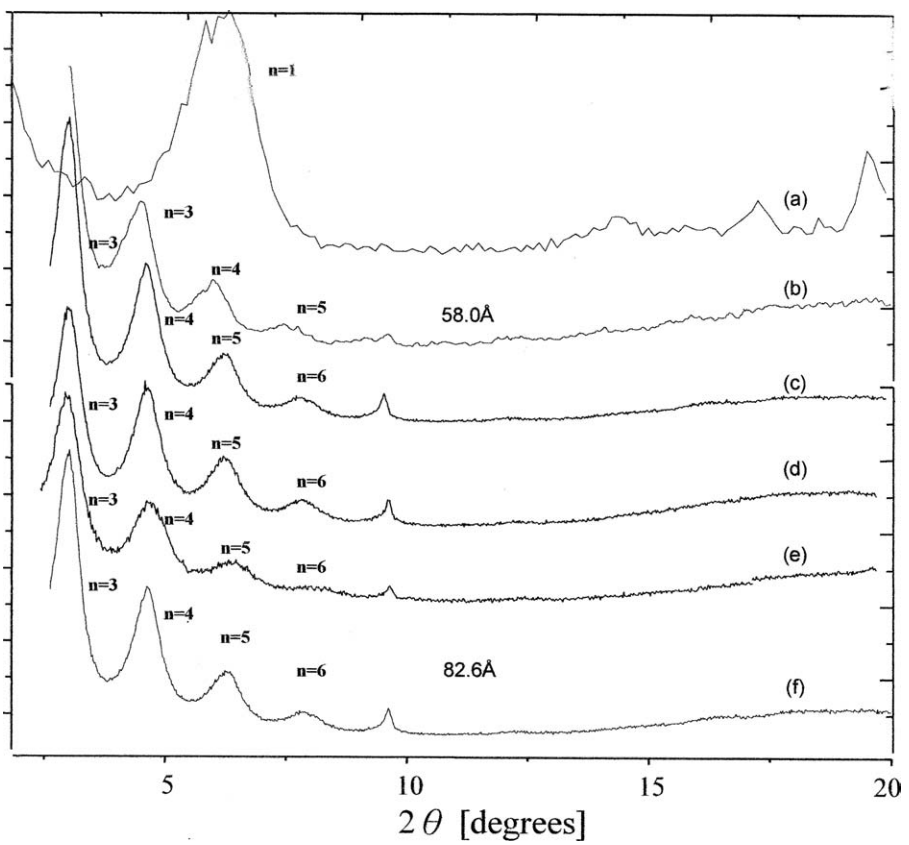

Figure 4 XRD patterns of (a) 1/1 Cu(II)/MMT, (b) 1/1 POP/MMT, (c) 1/0.1/1 POP/Cu(II)/MMT, (d) 1/0.3/1 POP/Cu(II)/MMT, (e) 1/0.5/1 POP/Cu(II)/MMT, and (f) 1/1/1 POP/Cu(II)/MMT.

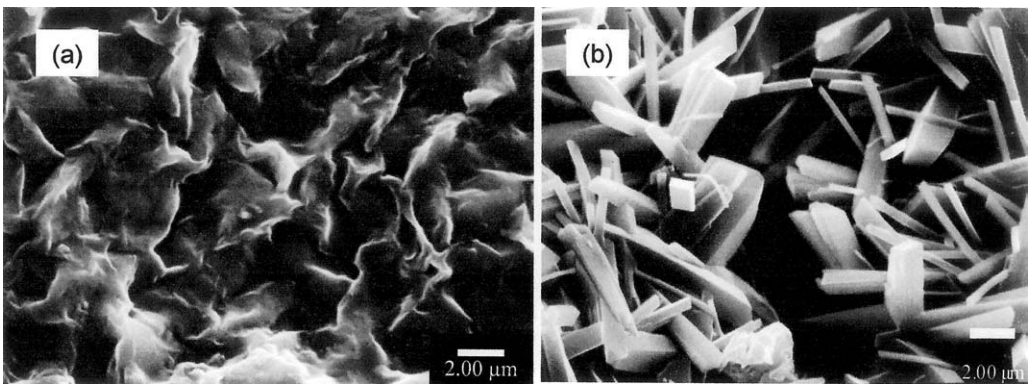

Figure 5 SEM images of (a) flakelike POP/MMT aggregates and (b) layer-stacking POP/Cu(II)/MMT crystals on (001).

= 3–6 represented the secondary structure in the presence of Cu(II).

Osmotic pressure applied to the organoclay

Increasing the Cu(II) loadings enlarged the *d*-spacing further for the range 0.1–1.0 CEC, but the *d*-spacing collapsed with 5–33 CEC surplus additions. The XRD diffraction patterns with POP with 1.0 CEC and Cu(II) at 0.1, 0.3, 0.5, and 1.0 CEC simultaneous intercalation are compared in Figure 4. The addition of Cu(II) rendered a heterogeneous nucleating effect on the (001) plane and favored the layer-stacking crystal form, with the explanation that osmotic pressure was applied on the organoclay wide surface. The microscopic crystallization forms of POP/MMT and POP/Cu(II)/MMT are shown in Figure 5. Compared to the random aggregation of POP/MMT,[22] the layered silicates, Cu(II) may have intercalated and increased the formation of face-to-face self-assemblies. The intercalated silicates enabled the formation of an orderly column texture that was a secondary structure self-aligned from the POP/Cu(II)/MMT primary units. The self-assembly was derived from an alignment force.[19] In the POP/Cu(II)/MMT primary units, the van der Waals force of polymers attached on the silicate surface rendered a function for the alignment of the individual units.

n for Cu(II)/MMT was 1, and it increased to 5 for the POP/MMT composite. Furthermore, the addition of Cu(II) to POP/MMT increased *n* to 6. The intensity in the sequential pattern for the high *n* value in the (001) direction is shown in Figure 6. The values of *n* were not altered with increasing Cu(II) loadings until the breaking point at surplus addition. The depletion aggregation was initiated at 0.1 equiv (or 1.6 wt %) and was maintained in the range 0.1–1.0 equiv ratio.

The POP molecules, salt ions, and water molecules were located in the interlayer regions between regularly spaced clay platelets. An approximately 70-Å thickness of polymeric complex formed a solid depletion layer on the surface, which was assumed to be equal to the gallery height of the intercalated clay and equal to the *d*-spacing of 80 Å of 1.0/0.5 POP/Cu(II) to the substrate of the single silicate layer thickness in 10 Å. The polymer segments that were not adsorbed onto the clay surfaces were rather homogeneously distributed in the interlayer region, at least in this case with a high-molecular-weight POP. Each polymer molecule was adsorbed onto both clay surfaces and, thereby, induced a reduction of the interlayer spacing by a phenomenon known as *polymer bridging flocculation.*[3–6] The interaction between the clay layers and the polymer changed its crystalline morphology. The crystal formation suggested that the induced clay surface kinetically favored the formation of a nematic phase.

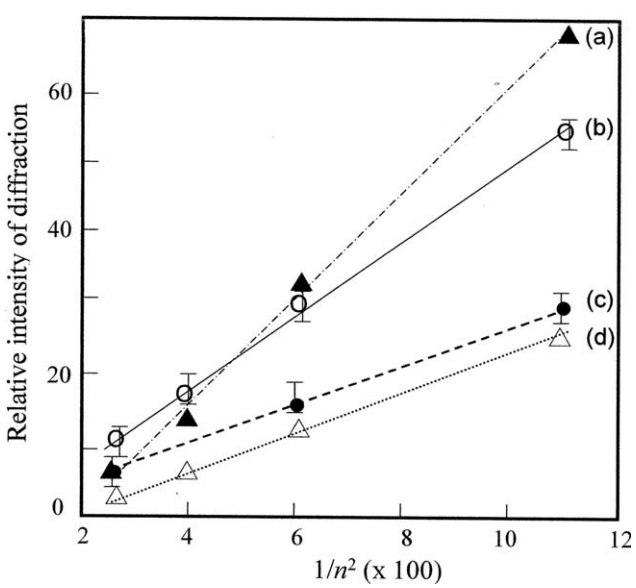

Figure 6 Relative intensity of XRD as function of *n* for (a) 1/0.5/1 POP/Cu(II)/MMT, (b) 1/1/1 POP/Cu(II)/MMT, (c) 1/1 POP/MMT, and (d) 1/0.1/1 POP/Cu(II)/MMT.

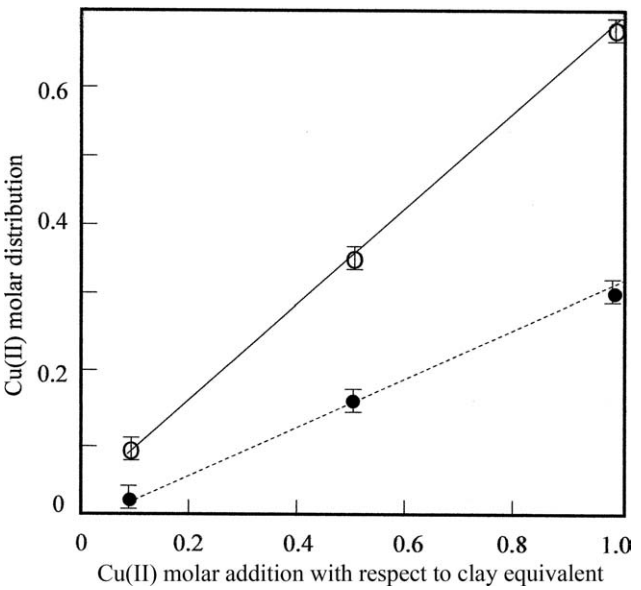

Figure 7 Cu(II) distribution in (○) the solid phase and (○) the liquid phase.

Symmetry breakdown of the organoclay

The osmotic pressure enforced on the organosilicate aggregation should have been proportional to the dissolved concentration of Cu(II) ions. The portion of Cu(II) was adsorbed into the solid phase of organoclay and was measured by element analysis, as shown in Table II. The ratio of the dissolved part was calculated by the following equation:

$$\text{Cu(II) in the liquid phase} = \text{Total Cu(II) addition} - \text{Intercalated Cu(II)} \quad (6)$$

Cu(II) was added to the POP/clay solutions at 0.1, 0.5, and 1.0 equiv, and after the ion-exchange experimental process, 0.08, 0.34, and 0.68 ratios were found to be adsorbed into the silicate, as measured by copper elemental analysis (Table II). Cu(II) ion in solution was compared with that absorbed by the solid, as shown in Figure 7. Approximately, 20–30 mol % total Cu(II) addition in the liquid phase was estimated to affect the formation of crystalline structure. Consequently, high epitaxial stacking in the formation of the secondary crystal structure in the (001) direction was observed. The osmotic pressure (π) is function of the concentration of solute:

$$\pi = (m/v)RT \quad (7)$$

where m/v is the molar concentration of the solute, R is the gas constant, and T is the absolute temperature. Therefore, the osmotic pressure was proportional to the Cu(II) ion molar concentration in the liquid phase. The relative pressure force exerted on the silicate gallery was calculated directly from the Cu(II) molar concentration in the liquid phase. The osmotic pressure effect on d-spacing is shown in Figure 8; as the osmotic pressure increasingly built with Cu(II) addition, the d-spacing suddenly collapsed to 18 Å.

The strongly reduced d-spacing was due to the phenomenon of depletion breakdown. As the osmotic pressure was exerted by the surplus salt content in the liquid, the conformation of the polyether flexible coil could no longer sustain its δ. The organoclay packing symmetry was, hence, destroyed, and the d-spacing dropped. The intensities of the higher order of Bragg's peaks are particularly sensitive to the scattering uniformity of reflection. n decreased from 6 for the 1/1 POP/Cu(II) intercalated MMT to only 1 for the POP/Cu(II) with a ratio of around 1.4. This was interpolated from Table II and Figure 8, and the random aggregation structure of the 1.0/1.65 POP/Cu(II) is shown in Figure 9(a). This indicated that the symmetry on (001) decayed to a disordered structure and changed the aggregation morphology to large flakes.

Although the d-spacing shrunk tremendously, the polymer content in the hybrid remained relatively stable. This result implies that the persistent length of polymer conformation became shorter with Cu(II) ions in the cell gap of the interlayer after they exceeded a critical amount. The interlayer distance was functionalized as the backbone chain length with POP intercalation as $d = 2R_g$. The cationic polymer coil was confined in the interlayered silicate space and also absorbed on the corona surface of the primary particle, with an adhering force of ion bridges between the polymeric ammonium and clay plate surface, and could not easily be extracted out

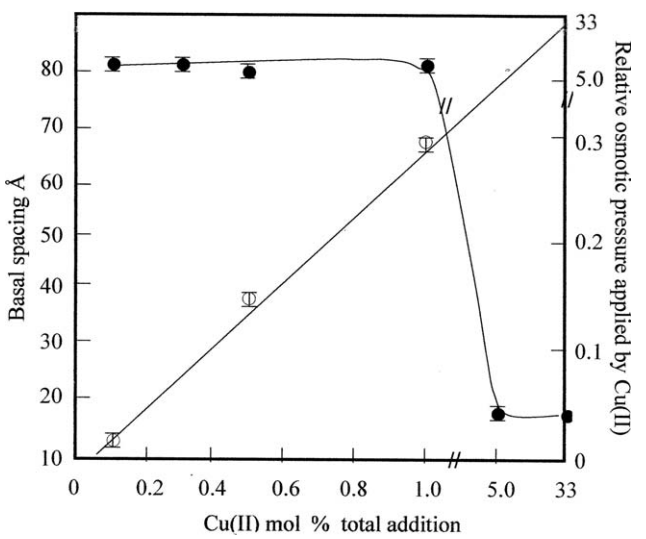

Figure 8 (●) d-spacing with respect to the buildup of the Cu(II) molar distribution and (○) relative osmotic pressure in the liquid phase.

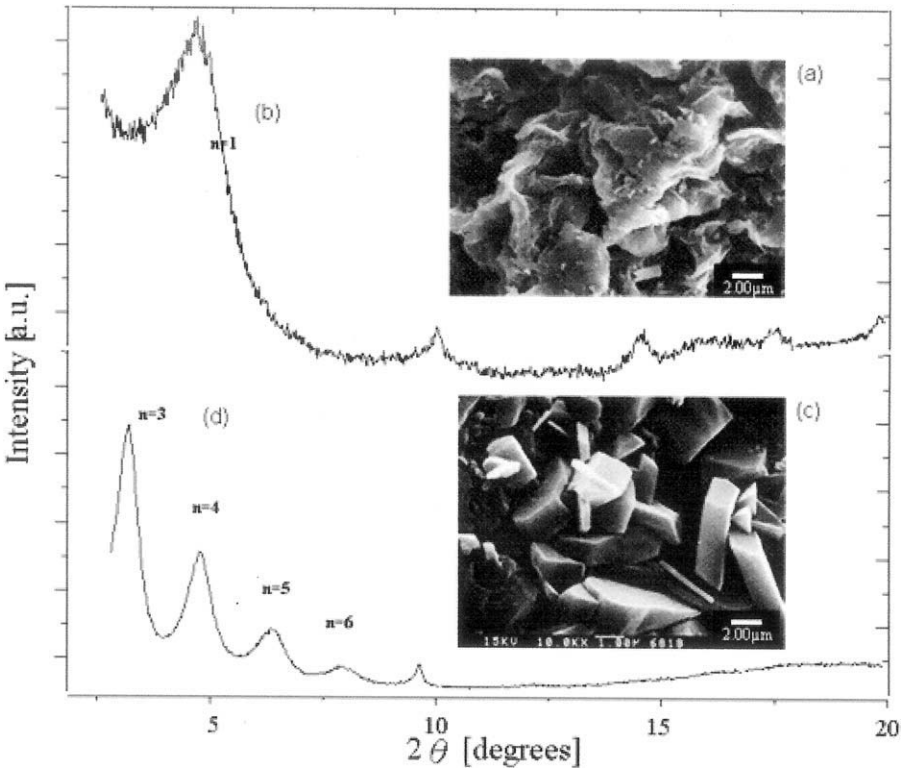

Figure 9 (a) Random aggregation of composites, (b) first-order XRD pattern for 1/1.65 POP/Cu(II) intercalated into MMT, (c) SEM image, and (d) high-order Bragg's pattern for 1/1 POP/Cu(II) in MMT.

of cells. The electrostatic interaction between the polyether and charged Cu(II) ions made the bond length shorter, and the microscopic order texture of the MMT platelets lost its support from the polymer pillar.

The depletion behavior of POP/Cu(II)/MMT revealed that pristine Cu(II) exerted a heterogeneous nucleating effect on the organoclays at 0.1–1.0 CEC, with the (001) crystal phase being preferentially nucleated. This was evidenced by the orders of increase in the X-ray reflection and crystalline dimensions [Fig. 9(c,d)]. The effect was related to the surface anchored with POP and uniformly extended molecular conformation. The intensity of the XRD crystalline-symmetry-sensitive diffractogram confirmed that the formation of the (001) crystalline phase was favored as Cu(II)/POP was involved. In contrast to the case of self-assembling crystallization, however, the surplus addition of Cu(II) changed the conformation of the polymer, as indicated in the XRD patterns. The (001) symmetry of interparticles was destroyed, and random aggregation was accompanied by the corresponding appearance of a broad Bragg's peak, as observed with Cu(II) addition exceeding 1.4 CEC [Fig. 9(a,b)].

CONCLUSIONS

In this study, a three-component system consisting of silicate, inorganic salt, and poly(ether amine) was generated to determine the mechanism of the depletion layer in layered clay. Through ionic exchange intercalation, cationic MMT units were modified and showed a correlation between the XRD Bragg's diffraction pattern with the crystallization and morphology of the clay aggregates. Macroscopic stacking to form new crystalline aggregates was found when the MMT was modified with an appropriated amount of POP salt/Cu(II). In contrast, an organoclay aggregate with a nonordered morphology was caused by electrostatic attraction between the positive edge and the negative surface. The addition of Cu(II) favored nucleation, which led to increasing bulk crystallization in the (001) plane and resulted in much larger crystals and a higher degree of crystallinity. Furthermore, a surplus addition of Cu(II) exerted an osmotic force on the silicate plates; this forced narrowing in the POP-supported silicate gallery and the disappearance of the self-assembled morphology.

References

1. Tuinier, R.; Rieger, J.; de Kruif, C. G. Adv Colloid Interface Sci 2003, 103, 1.
2. Schwarz, S.; Lunkwitz, K.; Keßler, B.; Spiegler, U.; Killmann, E.; Jaeger, W. Colloids Surf A 2000, 163, 17.
3. Zhivkov, A. M. J Colloid Interface Sci 2007, 313, 122.
4. Vincent, B. Colloid Surf 1990, 50, 241.
5. de Gennes, P. G. Macromolecules 1981, 14, 1637.

6. Tuinier, R.; Vliegenthart, G. A.; Lekkerkerker, H. N. W. J Chem Phys 2000, 113, 10768.
7. Odiachi, P. C.; Prieve, D. C. Colloids Surf A 1999, 146, 315.
8. Egger, H.; McGrath, K. M. Colloids Surf A 2006, 275, 107.
9. Vrij, A. Colloids Surf A 2003, 213, 117.
10. Seebergh, J. E.; Berg, J. C. Langmuir 1994, 10, 454.
11. Gordon, V. D.; Chen, X.; Hutchinson, J. W.; Bausch, A. R.; Marquez, M.; Weitz, D. A. J Am Chem Soc 2004, 126, 14117.
12. McFarlane, A.; Bremmel, K.; Addai-Mensah, J. J Colloid Interface Sci 2006, 293, 116.
13. Fuchs, M.; Schweizer, K. S. Europhys Lett 2000, 51, 621.
14. Netza, R. R.; Andelmanc, D. Phys Rep 2003, 380, 1.
15. Ray, S. S.; Okamoto, M. Prog Polym Sci 2003, 28, 1539.
16. Liu, P. Appl Clay Sci 2007, 38, 64.
17. Gilman, J. W. Appl Clay Sci 1999, 15, 31.
18. Ogata, N.; Kawakage, S.; Ogihara, T. Polymer 1997, 38, 5115.
19. Kawasumi, M.; Hasegawa, N.; Kato, M.; Usuki, A.; Okada, A. Macromolecules 1997, 30, 6333.
20. Hasegawa, N.; Okamoto, H.; Kawasumi, M.; Usuki, A. J Appl Polym Sci 1999, 74, 3359.
21. Muzny, C. D.; Butler, B. D.; Hanley, H. J. M.; Tsvetkov, F.; Peiffer, D. G. Mater Lett 1996, 28, 379.
22. Lin, J. J.; Cheng, I. J.; Wang, R.; Lee, R. J. Macromolecules 2001, 34, 8832.
23. Powell, C. E.; Beall, G. W. Curr Opin Solid State Mater Sci 2006, 10, 73.
24. Alexandre, M.; Dubois, P. Mater Sci Eng 2000, 28, 1.
25. Tjong, S. C. Mater Sci Eng Rep 2006, 53, 73.
26. Gabriel, J. C. P.; Sanchez, C.; Davidson, P. J Phys Chem 1996, 100, 11139.
27. Carrado, K. A. Appl Clay Sci 2000, 17, 1.
28. Pereira, C.; Patrício, S.; Silva, A. R.; Magalhães, A. L.; Carvalho, A. P.; Pires, J.; Freire, C. J Colloid Interface Sci 2007, 316, 570.
29. Petit, S.; Righi, D.; Madejová, J. Appl Clay Sci 2006, 34, 22.
30. Sobolewski, A. L.; Domcke, W. J Phys Chem 2002, 106, 4158.
31. Tombácz, E.; Szekeres, M. Appl Clay Sci 2006, 34, 105.
32. Lin, J. J.; Chou, C. C.; Lin, J. L. Macromol Rapid Commun 2004, 25, 1109.
33. Lin, J. J.; Chen, Y. M. Langmuir 2004, 20, 4261.
34. Lin, J. J.; Chu, C. C.; Chou, C. C.; Shieu, F. S. Adv Mater 2005, 17, 301.